Available online at www.sciencedirect.com
SCIENCE DIRECT®
Journal of Solid State Chemistry 175 (2003) 88–93
JOURNAL OF SOLID STATE CHEMISTRY
http://elsevier.com/locate/jssc

Structural, thermal and magnetic characterization of the manganese oxyhalide layered perovskite, $(MnCl)LaNb_2O_7$

Liliana Viciu, Vladimir O. Golub, and John B. Wiley*

Department of Chemistry and the Advanced Materials Research Institute, University of New Orleans, 2000 Lakeshore Drive, New Orleans, LA 70148-2820, USA

Received 7 December 2002; received in revised form 25 February 2003; accepted 28 February 2003

Abstract

Mn-Cl sheets were inserted into the perovskite blocks of a double-layered Dion–Jacobson compound by ion exchange at low temperature (390°C). The Rietveld structural analysis of X-ray powder diffraction data ($P4/mmm$) indicates that the product, $(MnCl)LaNb_2O_7$, has the manganese coordinated by two apical oxygens from the perovskite layers and four in-plane chlorines within the interlayer space. On heating, this compound exhibits an exothermic transition between 650°C and 750°C that is consistent with metastability. Magnetic characterization shows Curie–Weiss behavior at higher temperatures (>200 K) with a magnetic moment corresponding to the presence of high-spin Mn^{2+} ion ($S = 5/2$). At lower temperatures, antiferromagnetic interactions become significant and the broad maximum at 63 K reveals the 2-D character of the magnetic behavior. The susceptibility data, fit with the high temperature expansion for a Heisenberg square planar system, show a negative exchange interaction of $J/k = -3.77$ K.

Keywords: Layered perovskite; Metastable; 2-D Heisenberg magnetism

1. Introduction

Among the several materials derived from the perovskite structure, the Ruddlesden–Popper (RP) phases [1], $A_2[A'_{n-1}B_nO_{3n+1}]$, and Dion–Jacobson (DJ) layered phases [2], $A[A'_{n-1}B_nO_{3n+1}]$ (A = alkali metal, A' = rare earth, B = transition metal, n = the number of perovskite layers), are of great interest especially for their ability to undergo topochemical reactions [3]. These compounds have as a common feature the perovskite sheets $[A'_{n-1}B_nO_{3n+1}]$ separated by ion exchangeable A cations. The major difference in these phases is the number of alkali metals A in the interlayer. DJ compounds compared to RP phases have lower charge density and lower interlayer covalency—these features make them attractive for ion exchange [4], intercalation [5] and exfoliation reactions [6].

Recently we have reported on the assembly of metal-halide layers within DJ perovskites [7]. This chemistry is effective with a number of first-row transition-metal [8] and perovskite-host combinations [9]. Compounds of the general form $(MX)LaNb_2O_7$ (M = V, Cr, Mn, Fe, Co, Cu for X = Cl and M = Cu for X = Br) for example have been readily prepared [7,8]. An especially interesting member of the series is $(MnCl)LaNb_2O_7$. This low-temperature, low-dimensional phase exhibits unusual physical properties. Our initial report on this compound focused mostly on preparation [8], herein we present a thorough treatment of its structural, thermal and magnetic behavior.

2. Experimental section

2.1. Synthesis

$(MnCl)LaNb_2O_7$ was topotactically obtained from the DJ phases, $ALaNb_2O_7$, A = Na, Li. First, $RbLaNb_2O_7$ was prepared from La_2O_3 (Alfa, 99.99%), Nb_2O_5 (Alfa, 99.9985%) and Rb_2CO_3 (Alfa, 99%) by methods similar to that reported in Refs. [8,10]. The La_2O_3 was heated at 1050°C for 16 h in order to remove any carbonate or water impurities. Stoichiometric

*Corresponding author. Fax: +1-504-280-6860.
E-mail address: jwiley@uno.edu (J.B. Wiley).

0022-4596/03/$ - see front matter © 2003 Elsevier Science (USA). All rights reserved.
doi:10.1016/S0022-4596(03)00186-5

quantities of La_2O_3 and Nb_2O_5 with a 25% molar excess of Rb_2CO_3 were ground together, annealed for 12 h at 850°C followed by an additional thermal treatment at 1050°C for 24 h. The excess of Rb_2CO_3 was added to balance that lost due to volatilization. The product was washed with distilled water and dried at 150°C overnight. Both $LiLaNb_2O_7$ and $NaLaNb_2O_7$ were obtained by ion exchange reactions from the corresponding nitrates and $RbLaNb_2O_7$ in 10:1 molar ratio at 300°C and 400°C, respectively. After 24 h, the products were thoroughly washed with warm water and acetone and then dried at 150°C for 4 h. Single-phase $NaLaNb_2O_7$ was obtained after three cycles of treatment in molten salt.

To prepare $(MnCl)LaNb_2O_7$, $ALaNb_2O_7$ (A = Li, Na) were mixed with 2-fold molar excess of ultra dry $MnCl_2$ (Alfa, 99.99%) and then pressed into pellets with a hand press inside an argon-filled glove box. Reactions were carried out in a sealed, evacuated ($<10^{-3}$ Torr) Pyrex tube at 390°C for 7 and 9 days for the lithium and sodium hosts, respectively. Products were washed with water and acetone to eliminate the excess manganese chloride and the alkali-metal byproduct. $(MnCl)LaNb_2O_7$ is beige in color. Incomplete ion exchange reactions were observed when $RbLaNb_2O_7$ was used as the host.

2.2. Characterization

The product was insoluble in a variety of acids even after exposure to acidic solutions for long periods of time. Elemental analysis was therefore carried out by energy dispersive spectroscopy (EDS) on a series of individual crystallites on a JEOL (model JSM-5410) scanning electron microscope (SEM) equipped with an EDAX (DX-PRIME) microanalytical system.

X-ray powder diffraction data were collected on a Philips X-Pert PW 3020 MPD X-ray diffractometer equipped with a graphite monochromator and Cu$K\alpha$ ($\lambda = 1.5418$ Å). The pattern was recorded in step-scanning mode between 20° and 110° 2θ with 0.02° step width and 10 s count time. The structure model was refined by the Rietveld method with the GSAS set of programs [11]. The refined parameters were: scale factor, zero-point shift, background parameters, peak shape parameters, cell parameters, atomic coordinates, site occupancies for manganese and chlorine and preferred orientation. The R factor (R_p), the weighted R factor (R_{wp}), and χ^2 are defined as profile, $R_p = \sum[y_{io} - y_{ic}]/\sum y_{io}$; weighted profile, $R_{wp} = [\sum w_i(y_{io} - y_{ic})^2/\sum w_i(y_{io})^2]^{1/2}$ and goodness of fit (GOF), $\chi^2 = [R_{wp}/R_{exp}]^2$. $R_{exp} = [(N-P)/\sum w_i y_{io}^2]^{1/2}$, y_{io} and y_{ic} are the observed and calculated intensities, w_i is the weighting factor, N is the total number of y_{io} data when the background is refined, and P is the number of adjusted parameters.

The stability of the product was investigated both by thermogravimetric analysis (TGA) on a TA Instruments Thermal Analyst-2000 system and by differential scanning calorimetry (DSC) with a Nietzsche 404S instrument. Samples were heated to 1000°C with a 10°C/min ramp in reducing (mixture of 8% hydrogen and 92% argon), oxidizing (oxygen), and inert (argon) atmospheres.

Magnetic susceptibility measurements were carried out with a superconducting quantum interference device (SQUID) magnetometer (Quantum Design, MPMS-5S) over the temperature range 3–300 K in a field of 100 G.

3. Results

3.1. Synthesis

The ability of the DJ series $ALaNb_2O_7$ (A = Li, Na, K, Rb) to undergo ion exchange reactions with manganese chloride was investigated. Single-phase $(MnCl)LaNb_2O_7$ could only be obtained from lithium and sodium compounds. The reaction time varies slightly as a function of host, occurring the fastest with the lithium compound; reactions with lithium compound went to completion in 7 days at 390°C, while those with sodium were complete after 9 days. The chemical analysis of the carefully washed sodium product shows the Mn:Cl:La:Nb ratio of approximately 0.94(1):0.91(9):1:2.17(4).

3.2. Structure

All the reflections in the $(MnCl)LaNb_2O_7$ X-ray powder pattern were indexed on a tetragonal cell. Cell parameters are given in Table 1. As is typical for metal-halide insertion reactions, an expansion in the c-axis, ca. 0.9 Å relative to $RbLaNb_2O_7$, is observed. Structural analysis was carried out by Rietveld refinement on a model similar to that reported for $(CuCl)LaNb_2O_7$ in the space group $P4/mmm$ [7,14]. The basic structure consisted of manganese cations in D_{4h} symmetry surrounded by four coplanar chlorines and bridging

Table 1
Tetragonal unit cell parameters for the parents and the exchange product

Compound	Unit cell (Å)	Cell volume (Å)
$LiLaNb_2O_7$[a]	$a = 3.8798(1)$, $c = 20.3597(5)$	306.47
$NaLaNb_2O_7$[a,b]	$a = 3.9022(1)$, $c = 21.1826(8)$	322.55
$RbLaNb_2O_7$[c]	$a = 3.896(9)$, $c = 11.027(2)$	167.4
$(MnCl)LaNb_2O_7$	$a = 3.900(2)$, $c = 12.019(7)$	182.8

[a] Ref.[12].
[b] Ref.[13].
[c] Ref.[7].

between apical oxygens of adjacent perovskite slabs. Because the thermal parameters for the manganese and chlorine were large, other models that included disorder of manganese and/or chlorine were also investigated. In the copper and iron systems, such models proved effective [7,14,15]. In the case of manganese, however, none of these models resulted in any improvement, neither in the agreement factors nor in the thermal parameters. The observed, calculated and difference plots for Rietveld refinement of $(MnCl)LaNb_2O_7$ are shown in Fig. 1. The corresponding structural parameters are presented in the Table 2. A slight deviation from stoichiometry for Mn and Cl in the structure was found which is consistent with analytical data. The structural model is shown in Fig. 2 and the bond distances of manganese–anion and niobium–oxygen as well as lanthanum–oxygen are provided in Table 3.

3.3. Thermal analysis

$(MnCl)LaNb_2O_7$ was studied by thermogravimetric analysis and differential scanning calorimetry in oxygen, argon and hydrogen. From TGA, the resulting curves indicated that $(MnCl)LaNb_2O_7$ starts to decompose at $\sim$650°C. The total weight loss in oxygen and argon ($\sim$4.3%) differs from that in hydrogen ($\sim$5.4%). Elemental analysis and X-ray powder diffraction were carried out on the residue mixtures; EDAX showed that the compound completely loses all its chlorine in all cases and XRD analysis indicated the presence of $LaNbO_4$, $MnNb_2O_6$, and $MnNbO_4$. DSC analysis of $(MnCl)LaNb_2O_7$ (Fig. 3) exhibited an irreversible exothermic event at $\sim$670°C in hydrogen, $\sim$700°C in argon, and $\sim$730°C in oxygen.

3.4. Magnetism

The variation in magnetic susceptibility as a function of temperature is shown in Fig. 4. Because no difference in zero-field-cooled (ZFC) and field-cooled (FC) was observed, only ZFC data are presented here. The susceptibility values increase as the temperature decreases until a maximum is reached at about 63 K. At lower temperatures ($T<40$ K), a small Curie tail is observed. The compound is paramagnetic above 200 K and follows the Curie–Weiss law with $C = 4.467(2)$ emu K/mole and $\theta = -145.7(1)$ K. The calculated magnetic moment from the fitted data (inset in Fig. 4) is $\mu_{eff} = 5.9\,\mu_B$ per formula unit of $(MnCl)LaNb_2O_7$. The value is in good agreement with the observed magnetic moments for an ion in high-spin d^5 configuration [16].

4. Discussion

The synthesis of $(MnCl)LaNb_2O_7$ is achieved by a simple ion exchange reaction,

$$A LaNb_2O_7 + MnCl_2 \rightarrow (MnCl)LaNb_2O_7 + ACl,$$

where A = Li, Na. Similar reactions with $RbLaNb_2O_7$ also form $(MnCl)LaNb_2O_7$, but are incomplete even after reacting for over 2 weeks. In contrast, $(CuX)LaNb_2O_7$ (X = Cl, Br) and some other metal chlorides can be readily prepared from the Rb containing host. This variation likely relates to transition-metal and alkali-metal cation mobilities; though no data is available on the mobilities of the transition metals in these systems, Sato et al. and others [12,17] have reported on the relative mobilities of alkali metal cations within the DJ type layered perovskites and clearly show that lithium and sodium cations are more mobile than some larger alkali metals.

The $(MnCl)LaNb_2O_7$ structure is similar to other transition-metal oxyhalide exchange products; [7,15] the perovskite framework is preserved during the reaction, with the newly inserted transition-metal cations bridging between two perovskite layer apical oxygens and four equatorial chlorines $[MO_2Cl_4]$. Differences are seen however in the details of the metal-cation octahedra. In $(CuCl)LaNb_2O_7$, the $[CuO_2Cl_4]$ octahedra are distorted—four short bonds and two long—as a result of the Jahn–Teller effect, [7,14] and in $(FeCl)LaNb_2O_7$ the

Table 2
Crystallographic data for $(MnCl)LaNb_2O_7$

Atom	Site	x	y	z	g[a]	U_{iso} (Å^2)
Mn	1*d*	1/2	1/2	1/2	0.969(9)	0.042(2)
Cl	1*b*	0	0	1/2	0.92(1)	0.032(4)
La	1*a*	0	0	0	1	0.0158(5)
Nb	2*h*	1/2	1/2	0.1894(1)	1	0.0155(6)
O1	4*i*	0	1/2	0.1655(5)	1	0.031(2)
O2	2*h*	1/2	1/2	0.3179(9)	1	0.047(5)
O3	1*c*	1/2	1/2	0	1	0.062(6)

$P4/mmm$, $Z = 1$, $R_p = 13.35\%$, $R_{wp} = 18.76\%$, $\chi^2 = 1.563$.
[a] g = occupation factor.

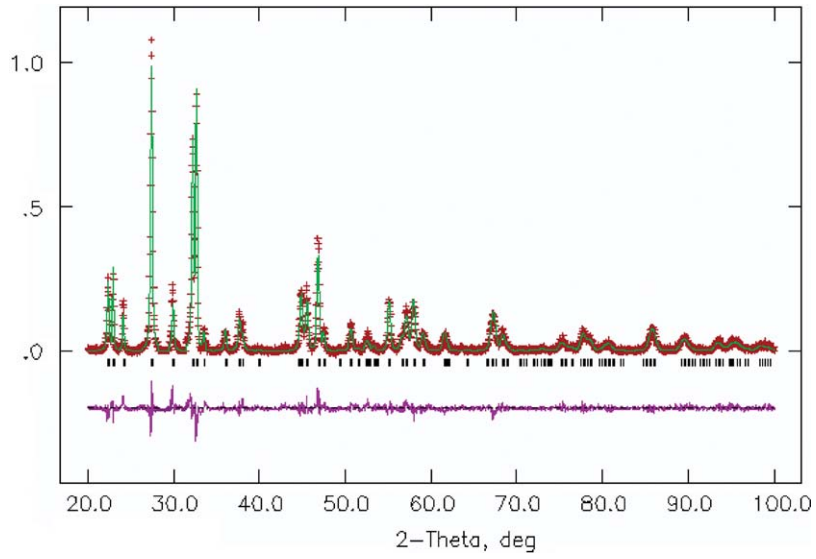

Fig. 1. Experimental, calculated, and difference X-ray powder patterns for the Rietveld refinement of $(MnCl)LaNb_2O_7$.

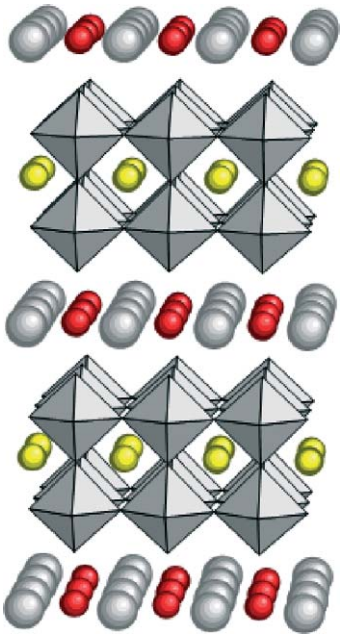

Fig. 2. The structure of $(MnCl)LaNb_2O_7$: the octahedra represent NbO_6, the spheres within perovskite layers are lanthanum ions, between the layers the smaller dark spheres are manganese ions while the larger ones are the chlorine ions.

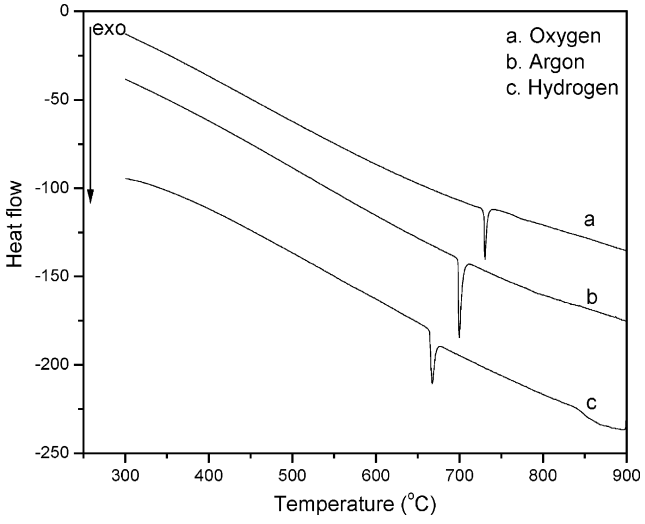

Fig. 3. The DSC curves for $(MnCl)LaNb_2O_7$ in oxygen, argon and hydrogen.

Table 3
Selected bond distances (Å) for $(MnCl)LaNb_2O_7$

Bond	Length (Å)
Mn–O2	2.19(1)
Mn–Cl	2.758(2)
Nb–O1	1.972(2)
Nb–O2	1.55(1)
Nb–O3	2.277(2)
La–O1	2.786(5)
La–O3	2.758(2)

metal itself moves off an ideal octahedral position favoring a tetrahedral-like distortion [15]. In the case of $(MnCl)LaNb_2O_7$, though the large thermal parameters for Mn and Cl indicate a distortion in this compound as well, efforts to model this behavior have been unsuccessful. It is possible that the disorder in this system is in fact random. The coordination of the MnO_2Cl_4 octahedra in $(MnCl)LaNb_2O_7$ is similar to that seen in hydrates of alkali-metal manganese (II) chlorides. For both the 1-D chains of β-$RbMnCl_3 \cdot 2H_2O$ and 0-D polyhedra of $K_2MnCl_4 \cdot 2H_2O$, [18] two axial oxygens and four equatorial chlorines coordinate manganese. With respect to bond distances, the Mn–O bond distances (2.188(9) Å) in $(MnCl)LaNb_2O_7$ are very

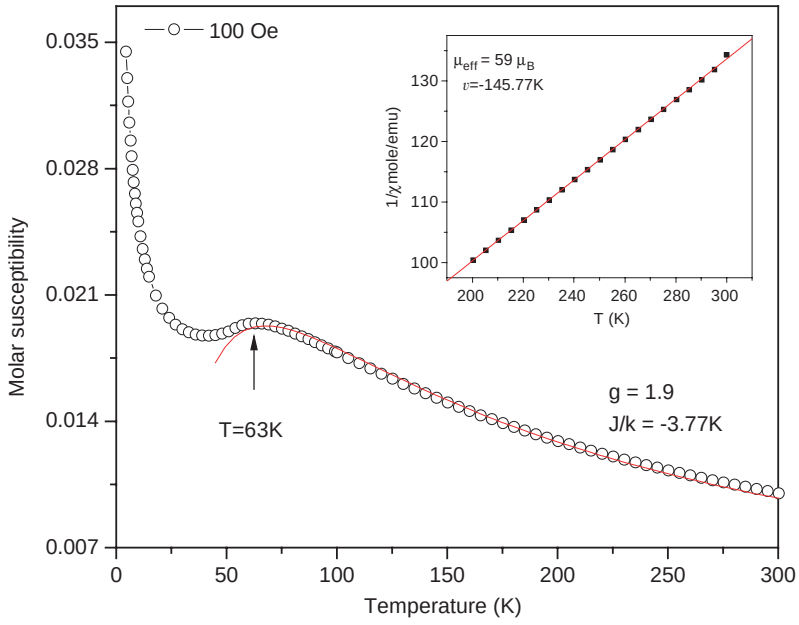

Fig. 4. Temperature dependence of the susceptibility at 100 G. The inset represents the reciprocal molar susceptibility between 100 and 300 K. Result of fitting a high-temperature expansion of the quadratic layer Heisenberg model to the data in the 54–300 K temperature range is shown as solid line.

similar to those of the hydrates (range: 2.175–2.228 Å), whereas the Mn–Cl distances (2.768(4) Å) are on average about 0.2 Å longer. Based on the average Mn–Cl distance of 2.537 Å seen in the hydrates, for a perfect match between the perovskite layer and the Mn–Cl layer, the a parameter in the perovskite host should be closer to 3.6 Å ($\sqrt{2} \times 2.537$ Å) not the 3.9 Å observed. The elongation of the Mn–Cl bond and the large thermal parameters observed for both manganese and chlorine may, therefore, reflect a poor "lattice match" between the two sublayers.

Thermal analysis shows that $(MnCl)LaNb_2O_7$ is a low temperature, metastable phase which decomposes above 650°C. EDAX and XRD on the final decomposition products indicate that the weight loss is primarily due to loss of chlorine, possibly as the diatomic gas, and that manganese is present as Mn(II) or Mn(III) in $MnNb_2O_6$ and $MnNbO_4$, respectively. This would suggest that the chlorine is being replaced by oxygen around the point of decomposition; similar behavior has been reported in this temperature range for other oxides [19]. The exotherm observed in DSC is presumably coming from the formation of $LaNbO_4$, both lanthanum and niobium in the $LaNb_2O_7^-$ layer have a higher coordination number [8]. The temperature of the exothermic event appears to depend on reaction atmosphere, where the event is suppressed the more oxidizing the gas. This likely indicates that oxygen and/or oxygen vacancies play some role in the decomposition mechanism. Overall the thermal behavior of $(MnCl)LaNb_2O_7$ is significant in that it indicates that compounds prepared by these topotactic routes are not likely accessible by standard ceramic techniques.

Magnetic data were modeled with the 2-D Heisenberg approach. The susceptibility data were fitted between 54 and 300 K with the high-temperature series expansion reported by Rushbrooke and Wood [20] for a 2-D Heisenberg square planar system (Fig. 4):

$$\chi = \frac{S(S+1)Ng^2\,\mu_B}{3kT} \sum_{n=0}^{6} (-1)^n \frac{b_n}{\theta^n},$$

where N is the Avogadro's number, k the Boltzmann constant, μ_B the Bohr magneton, $\theta = kT/J$, J the exchange constant and the b coefficients were calculated to be: $b_0 = 1$; $b_1 = -23.33$; $b_2 = 147.78$; $b_3 = -405.48$; $b_4 = 8171.3$; $b_5 = -64967.7$; $b_6 = 158110$. This model produced an exchange parameter of $J/k = -3.77$ K with a $g = 1.9$. Further, according to De Jongh and Miedema [21], the expressions describing a square planar Heisenberg model with $S = 5/2$ are: $kT(\chi_{max})/|J|S(S+1) = 2.05$ and $\chi_{max}|J|/Ng^2\mu_B^2 = 0.0551$. By taking in account the position of the temperature where the maximum of antiferromagnetic susceptibility occurs one can ascertain the intraplanar exchange constant. The J/k values for $(MnCl)LaNb_2O_7$ calculated from each of these expressions are −3.51 and −3.72 K, respectively. These values are in very close agreement with that observed from the experimental fitted data (−3.77 K). The exchange constants for some other two-dimensional Mn(II)-chloride layer compounds were found to vary between 4 and 6 K [22].

Also, the broad susceptibility maximum at 63 K is attributed to short range antiferromagnetic order. The Nèel temperature (T_N) can then be obtained by plotting $d\chi T/dT$; [23] a T_N of ca. 54 K was found in (MnCl)$LaNb_2O_7$. Finally, the Curie tail observed at low temperature is likely associated with the presence of isolated paramagnetic ions in the crystal; it is estimated that this would correspond to about 3% of the total manganese.

5. Conclusions

Low-temperature topotactic reactions can lead to the creation of metal-anion layers within receptive hosts. The compounds prepared by these methods can exhibit correlated magnetic properties. Further development of such reaction strategies, especially in combination with redox chemistry, should lead to other interesting anisotropic materials, possibly those exhibiting colossal magnetoresistance or superconductivity.

Acknowledgments

We gratefully acknowledge financial support from the National Science Foundation (DMR-9983591).

References

[1] S.N. Ruddlesden, P. Popper, Acta Crystallogr. 10 (1957) 538.
[2] M. Dion, M. Ganne, M. Tournoux, Mater. Res. Bull. 16 (1981) 1429;
A.J. Jacobson, J.W. Johnson, J.T. Lewandowski, Inorg. Chem. 24 (1985) 37.
[3] R. Schaak, T.E. Mallouk, Chem. Mater. 14 (2002) 1455 (and the references therein).
[4] A.J. Jacobson, J.W. Johnson, J.T. Lewandowski, Inorg. Chem. 24 (1985) 3729;
J. Gopalakrishnan, S. Uma, V. Bhat, Chem. Mater. 5 (1993) 132;
B.L. Cushing, J.B. Wiley, Mater. Res. Bull. 34 (1999) 271.
[5] R. Jones, W.R. McKinnon, Solid State Ion. 45 (1991) 173;
P. Gomez-Romero, M.R. Palacin, N. Casan, A. Fuerts, Solid State Ion. 63–65 (1993) 424;
A.R. Armstrong, P.A. Anderson, Inorg. Chem. 33 (1994) 4366.
[6] M. Fang, C.H. Kim, T.E. Mallouk, Chem. Mater. 11 (1999) 1519.
[7] T.A. Kodenkandath, J.N. Lalena, W.L. Zhou, E.E. Carpenter, C. Sangregorio, A.U. Falster, W.B. Simmons, C.J. O'Connor, J.B. Wiley, J. Am. Chem. Soc. 121 (1999) 10743.
[8] L. Viciu, G. Caruntu, N. Royant, J. Koenig, W.L. Zhou, T.A. Kodenkandath, J.B. Wiley, Inorg. Chem. 41 (2002) 3385.
[9] T.A. Kodenkandath, A.S. Kumbhar, W.L. Zhou, J.B. Wiley, Inorg. Chem. 40 (2001) 710.
[10] J. Gopalakrishnan, V. Bhat, Mater. Res. Bull. 22 (1987) 413.
[11] A. Larson, R.B. Von Dreele, GSAS: Generalized Structure Analysis System, Los Alamos National Laboratory, Los Alamos, NM, 1994.
[12] M. Sato, J. Abo, T. Jin, M. Ohta, J. Alloys Compd. 192 (1993) 81.
[13] M. Sato, J. Abo, T. Jin, Solid State Ion. 57 (1992) 285.
[14] G. Caruntu, T.A. Kodenkandath, J.B. Wiley, Mater. Res. Bull. 37 (2002) 593.
[15] L. Viciu, J. Koenig, L. Spinu, W.L. Zhou, J.B. Wiley, Chem. Mater. 15 (2003) 1480.
[16] C.J. O'Connor, Prog. Inorg. Chem. 29 (1982) 203.
[17] V. Thangadurai, P. Schmid-Beurmann, W. Weppner, J. Solid State Chem. 158 (2001) 279.
[18] S.J. Jenson, Acta Chem. Scand. 21 (1967) 889;
S.J. Jenson, Acta Chem. Scand. 22 (1968) 647.
[19] H. Schäfer Chemical Transport Reactions Academic Press, New York, 1964, p. 54.
[20] G.S. Rushbrooke, P. Wood, Mol. Phys. 6 (1963) 409.
[21] L.J. de Jongh, A.R. Miedema, Adv. Phys. 23 (1974) 1.
[22] R. Navarro, in: L.J. de Jongh (Ed.), Magnetic Properties of Layered Transition Metal Compounds, Kluwer Academic Publishers, Dordredcht, The Netherlands, 1990, p. 105 (and the references therein).
[23] M.E. Fisher, Am. J. Phys. 32 (1964) 343.